Stability and nesting of dissipative vortex solitons with high vorticity

B. N. Aleksić,[1,2] N. B. Aleksić,[1,2] V. Skarka,[1,2,3,*] and M. Belić[1]
[1]*Texas A&M University at Qatar, P.O. Box 23874, Doha, Qatar*
[2]*Institute of Physics, University of Belgrade, 11000 Belgrade, Serbia*
[3]*Laboratoire de Photonique d'Angers, EA 4464, Université d'Angers, 2 Boulevard Lavoisier, 49045 Angers Cedex 01, France*
(Received 11 May 2014; published 22 April 2015)

Using the variational method extended to dissipative systems and numerical simulations, an analytical stability criterion is established allowing the determination of stability domains of parameters for vortices with high topological charge S. Parameters from these domains are used as inputs for numerical self-generation of previously unexplored coexisting stable vortex solitons with topological charge ranging from $S = 3$ to $S = 20$. The nesting of low-vorticity solitons within those of higher vorticity is discovered. Such a self-organized structuring of light allows for selective dynamic nanophotonic tweezing.

DOI: 10.1103/PhysRevA.91.043832 PACS number(s): 42.65.Tg, 05.45.Yv, 42.65.Sf, 47.20.Ky

In general, external energy and/or matter supply in a nonlinear system provides for the emergence of self-organized dissipative structures far from the thermodynamic equilibrium [1]. The solitonic structures self-organization involves the balance of antagonistic effects: loss versus gain, diffusion against nonlinearity-induced self-contraction. Complex Ginzburg-Landau equations (GLEs) describe well the dissipative soliton generation in nanophotonics, plasmonics, fluids, plasmas, and electromagnetism, as well as superconductivity, superfluidity, elementary particles, and biological systems [2]. Various species of self-trapped localized structures are provided by acting as attractors [3]. In nonlinear optics and nanophotonics, solitons, described by nonlinear Schrödinger equation (NSE), are self-generated through the simultaneous balance of diffraction and/or dispersion by self-focusing. In two- and three-dimensional systems, the focusing cubic nonlinearity may lead to catastrophic collapse. In media having negative quintic nonlinearity in addition to the cubic one, such a collapse is prevented. Consequently, continuous families of stable spatial and spatiotemporal conservative solitons have been found as solutions of the nonlinear cubic-quintic Schrödinger equation (CQSE) [4,5]. The generation of two-dimensional (2D) optical solitons in a cubic-quintic medium has been recently directly demonstrated in an experiment [6]. In physically realistic systems omnipresent losses would destroy dissipative solitons if they are not compensated for by gain. Therefore, only the simultaneous balance of diffraction and dispersion by saturating nonlinearity as well as of loss by gain ensures the stability of dissipative solitons described by a multidimensional GLE [7]. As a consequence, for given sets of dissipative parameters the GLE solitons have isolated solutions [2].

Dissipative vortex structures with nonzero angular momentum have direct counterparts in nature (e.g., tornados). Vortex solitons are self-structured around zero intensity topological singularity at the center, described by the topological charge S [8,9]. Recently we found that dissipative vortices with vorticity $S = 1$ spontaneously break axial symmetry due to modulational instability. They either break into filaments or evolve into stably rotating ellipsoidal solitons [10]. It is considered that vortex structures with high topological charge S should be unstable due to the increase of modulational instability with the increase of vorticity [4]. Indeed, for higher vorticity the radius of the broad one-dimensional Gaussian laser beam in conservative systems is subject to strong modulational instability causing it to break into filaments [11]. Up to now, stable vortices were reported only up to $S = 5$ in conservative systems [12] and up to $S = 3$ for dissipative ones [13]. Hence, vortices with high charge S are commonly considered as unstable. Using synergy between the variational method extended to dissipative systems and exhaustive numerical simulations we were able to establish here the large domain of parameters in which dissipative vortex solitons with charge up to $S = 20$ are found stable. Moreover, dissipative vortex solitons with lower charge are nested within those with higher charge. Such a self-generated structured light may be used for different applications including selective dynamic nanophotonic tweezing.

Self-organization, propagation, and stability of dissipative vortex solitons can be adequately modeled by the 2D cubic-quintic (CQ) GLE that governs the evolution of a normalized complex envelope $E(z,r,\varphi)$ of electric waves in nanophotonic or plasmonic media

$$i\frac{\partial E}{\partial z} + \Delta E + |E|^2E - |E|^4E = \mathbb{Q}, \tag{1}$$

where $\Delta E = r^{-1}\partial/\partial r(r\partial E/\partial r) + 1/r^2\partial^2E/\partial\varphi^2$ is Laplacian describing laser beam diffraction. To prevent beam collapse, cubic and quintic nonlinearities have opposite signs. Dissipative terms are denoted by $\mathbb{Q}$

$$\mathbb{Q} = i\varepsilon|E|^2E + i\beta\Delta E - i\delta E - i\mu|E|^4E. \tag{2}$$

Positively defined dissipative parameters ε, δ, μ, and β characterize respectively cubic gain, linear, and quintic nonlinear losses, as well as field diffusion. The CGLE does not admit exact solutions, with rare exceptions [14]. Although one has to resort to numerical simulations, the variational approach (VA) providing approximated analytical solutions is essential in order to establish an analytical stability criterion helping numerical computations. Following Hamilton's principle $\delta(\int dz \int\int L_o r\,dr\,d\varphi) = 0$, the extremum function $E(z,r,\varphi)$ renders the Lagrangian integral stationary under

*vladimir.skarka@univ-angers.fr

the condition that the Euler-Lagrange equation corresponding to Eq. (1) $\sum_\xi d/d\xi(\partial L_o/\partial E_\xi) - \partial L_o/\partial E^* = 0$ holds ($\xi = z,r,\varphi$). However, such a standard VA has to be generalized to dissipative systems [7].

Using CQGLE we are investigating the propagation of a realistic singular Gaussian laser beam. As a consequence, the trial function has to be of Gaussian shape

$$E = \mathcal{A}\left(\frac{r}{\mathcal{R}}\right)^S [1 + U\cos(l\varphi)] \times \exp\left[-\frac{r^2}{2\mathcal{R}^2} + i\mathcal{C}r^2 + iS\varphi + i\Psi\right], \quad (3)$$

with the scaled amplitude $\mathcal{A} = A_* A(z)$, beam width $\mathcal{R} = R_* R(z)$, wave front curvature $\mathcal{C} = C(z)/R_*^2$, and phase $\Psi(z)$. The scaling factors are $R_* = (2/A_*)\sqrt{2^{2S}(S)!/(2S)!}$ and $A_* = (3/2)\sqrt{3^{3S}(2S)!/2^{2S+1}(3S)!}$. In order to check the influence of modulational instability with the increase of charge S, which is prone to destroy vortices, we introduce an azimuthal (angle φ) perturbation of order l with complex amplitude $U(z) = U_r(z) + iU_i(z)$. Following Kantorovitch, constant parameters of the Rayleigh-Ritz method are substituted here by functions η=$\mathcal{A}$, $\mathcal{R}$, $\mathcal{C}$, Ψ, U_r, U_i of propagation variable z [15]. Optimization of each of these functions gives one of six Euler-Lagrange equations

$$\frac{d}{dz}\left(\frac{\partial L}{\partial \eta'}\right) - \frac{\partial L}{\partial \eta} = 2\mathrm{Re}\int d\varphi \int \mathbb{Q}\frac{\partial E^*}{\partial \eta} r\, dr, \quad (4)$$

where Re denotes the real part [7]. The Lagrangian averaged over transverse coordinates r and φ is written as

$$L = \int d\varphi \int \left[\frac{i}{2}\left(\frac{\partial E^*}{\partial z}E - \frac{\partial E}{\partial z}E^*\right) + |\nabla E|^2 - \frac{1}{2}|E|^4 + \frac{1}{3}|E|^6\right] r\, dr. \quad (5)$$

The laser beam power

$$P = 2\pi \int |E|^2 r\, dr = 4\pi A^2 R^2 2^{2S}(S+1)!S!/(2S)! \quad (6)$$

is no more conserved in dissipative systems. By using the VA, through the optimization of all z-dependent functions, a system of Euler-Lagrange ordinary differential equations (ODEs) is obtained [7,16,17]:

$$\frac{dA}{dz} = \frac{1}{R_*^2}\left(\varepsilon(2S+3)A^2 - \frac{\mu(3S+5)A^4}{2} - 4C(S\beta R^2 C + 1) - \frac{\beta(S+2)}{R^2}\right)A - \delta A, \quad (7)$$

$$\frac{dR}{dz} = \frac{1}{R_*^2}\left(4RC - \varepsilon R A^2 + \mu R A^4 + \frac{\beta}{R} - 4\beta C^2 R^3\right), \quad (8)$$

$$\frac{dC}{dz} = \frac{1}{R_*^2}\left(\frac{1}{R^4} + \frac{A^4 - A^2 - 4\beta C}{R^2} - 4C^2\right), \quad (9)$$

$$\frac{dU_r}{dz} = \left(4\varepsilon A^2 - 6\mu A^4 - \frac{\beta\sigma^2}{R^2}\right)\frac{U_r}{T_*^2} + \frac{\sigma^2 U_i}{T_*^2 R^2}, \quad (10)$$

$$\frac{dU_i}{dz} = \left(4A^2 - 6A^4 - \frac{\sigma^2}{R^2}\right)\frac{U_r}{T_*^2} - \frac{\beta\sigma^2 U_i}{T_*^2 R^2}, \quad (11)$$

$$\frac{d\psi}{dz} = \frac{1}{T_*^2}\left[-\frac{2}{R^2} + 3A^2 - \frac{5}{2}A^4 + 4\beta C\right], \quad (12)$$

where $T_*^2 = R_*^2/(S+1)$. The ratio between the order l of azimuthal perturbation and the topological charge S is $\sigma = [l^2/S(S+1)]^{1/2}$.

Steady-state solutions are computed solving the set of ODEs, Eqs. (7)–(12) for vanishing derivatives. They correspond to fixed points with small nonzero wave-front curvature: $C = A^2[\varepsilon - \beta - (\mu - \beta)A^2]/4$ and radius $R = (A^2 - A^4)^{-1/2}$. In the dissipative case there are only two different steady-state solutions for the amplitude A: $A^\pm = \{[2\varepsilon - \beta \pm \sqrt{(2\varepsilon-\beta)^2 - T_*^2\delta(6\mu - 4\beta)}]/(3\mu - 2\beta)\}^{1/2}$. According to the general principles of the analysis of dissipative systems, A^+ solution may be stable, while A^- is always unstable [4,7]. The former solution satisfies the condition $C < 0$, which is necessary for the simultaneous self-organized cross-compensation between the gain and the loss, as well as the saturating CQ nonlinearity exceeding diffraction [7,16,17]. Such fixed points exist for a large domain of dissipative parameters. We established that their stability mainly depends on the dimensionless nonlinear gain parameter ε and the nonlinear loss parameter μ. Therefore, domains of existence of solutions for charges ranging from $S = 3$ to $S = 20$ are charted as functions of those two dimensionless dissipative parameters in Fig. 1 (shaded shell-like areas with darker

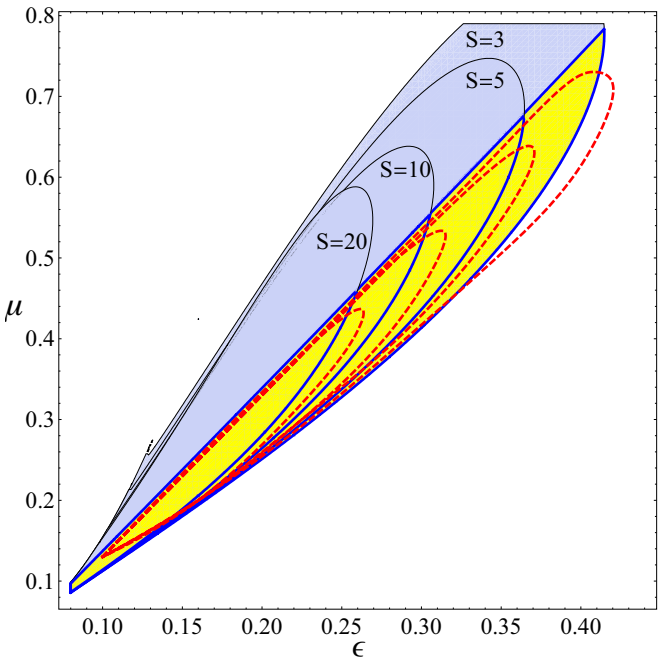

FIG. 1. (Color online) Stability domains produced by the VA-generated fixed points, in the plane of the nonlinear-gain strength, ε, and the nonlinear-loss strength, μ (both dimensionless). In the darker region fixed points are only radially stable, while in the brighter one they are also azimuthally stable. This is confirmed by direct simulations of Eq. (1) for parameters inside elliptic areas, delimited by dashed lines.

and brighter halves put together). Following our exhaustive numerical simulations the variation of the remaining two dissipative coefficients associated with linear loss (δ) and field diffusion (β) does not entail essential changes; only the shape of domains is slightly modified. Consequently, in order to adequately represent our main results we suitably choose $\delta = 0.01$ and $\beta = 0.05$. The realistic numerical values of dissipative parameters can be determined experimentally by the choice of laser beam intensity and the nonlinear active medium, e.g., by varying in laser cavity concentration of rhodamine dye in ethanol [18].

It is remarkable that the shaded shell-like areas in Fig. 1 of higher order vortices are nested (though not perfectly) within those of lower order, indicating their simultaneous coexistence. Indeed, the region corresponding to $S = 20$ is imbedded in the area of $S = 10$, which is a part of the $S = 5$ domain that belongs to the largest $S = 3$ region. We have checked also other values of charges, to conclude that all vortices up to $S = 20$ are nested within each other and simultaneously coexist in the smallest region of parameters, corresponding to the highest vorticity ($S = 20$). Steady-state solutions in shell-like areas are by no means all stable. Therefore, their stability has to be checked using the method of Lyapunov exponents [7,10,16,17]. Steady-state solutions of five coupled ODEs are stable following Lyapunov if and only if the real part of solutions λ of the equation $(\lambda^3 + \alpha_1\lambda^2 + \alpha_2\lambda + \alpha_3)(\lambda^2 + \alpha_5\lambda + \alpha_6) = 0$ is negative. Hence, Routh-Hurwitz conditions of positiveness of all coefficients of this equation must be satisfied $\alpha_1 = 2[\beta/R^2 + (3S + 5)\mu A^4 - (2S + 3)\varepsilon A^2]/R_*^2 > 0$, $\alpha_2 = 4A^2[2A^2+\beta(S+1)(\mu A^2 - \varepsilon)]/R_*^4R^2 > 0$, $\alpha_3 = 16(S+1)A^2[\beta - 2\varepsilon + A^2(3\mu - 2\beta)]/R_*^6R^4 > 0$, $\alpha_4 = \alpha_1\alpha_2 - \alpha_3 > 0$, $\alpha_5 = 2[(3\mu A^2 - 2\varepsilon)A^2 + \beta\sigma^2/R^2]/T_*^2 > 0$, and $\alpha_6 = \sigma^2[(1 + \beta^2)\sigma^2/R^2 + 6A^4(1 + \beta\mu) - 4A^2(1 + \beta\varepsilon)]/T_*^4R^2 > 0$. In this way the analytical stability criterion for all fixed points is established [7]. The positive coefficients α_1, α_2, α_3, and α_4 determine the radial stability of steady state solutions in whole shell-like stability domains in Fig. 1. However, in the darker half the coefficients α_5, α_6, determining azimuthal stability, are negative. Hence, although radially stable, vortices may break into filaments, due to the azimuthal modulational instability. Only in the brighter region are all coefficients positive, so the filamentation is prevented [7,10]. Therefore, only fixed points with parameters from the brighter regions in Fig. 1 are both radially and azimuthally stable; thus, they may become solitons during numerical self-organizing evolution.

Consequently, to generate dissipative vortex solitons, numerical propagation of Eq. (1) is performed with the input parameters coming from stable regions. Extensive parallelized numerical simulations are realized using graphical processing units (GPUs) [19]. Stable vortex solitons are self-generated for parameters inside elliptic areas, delimited by dashed lines in Fig. 1. These areas quite closely coincide with the analytically obtained stability regions confirming predictions following stability criterion.

Numerical results of a typical self-organizing evolution for the parameters $\mu = 0.4$ and $\varepsilon = 0.24$ from the stability regions are shown in Fig. 2 for topological charges $S = 3$ and $S = 5$ and in Fig. 3 for $S = 10$ and $S = 20$. The initial vortex at $z = 0$, which is not yet a soliton, is presented in the first panel of each tryptic, i.e., in Figs. 2(a), 2(d), 3(a), and 3(d), for the same input parameters confirming simultaneous coexistence. The vortex with charge $S = 3$ is numerically propagated for $z = 300$ units before becoming a stable dissipative vortex soliton [Fig. 2(b)]. For the next twenty thousand units this soliton stays unchanged [Fig. 2(c)]. As the topological charge increases, the crater of the initial vortex "volcano" enlarges, as in Fig. 2(d) for $S = 5$. The dissipative soliton for $S = 5$ is self-generated at $z = 500$ units [Fig. 2(e)]. Its stability was tested until $z = 20\,000$ [Fig. 2(f)]. The vortex soliton with doubled topological charge ($S = 10$) is self-organized at the doubled propagation distance $z = 1000$ [Fig. 3(b)] and it remains unchanged [see Fig. 3(c) for $z = 50\,000$]. Again, the doubling of the charge to $S = 20$ involves doubling propagation distance $z = 2000$ before a stable dissipative soliton is self-formed [Fig. 3(e)]. The robustness of this vortex soliton was tested up to $z = 80\,000$ [Fig. 3(f)]. Therefore, stable dissipative vortex solitons up to $S = 20$ predicted analytically are self-generated by numerical evolution after

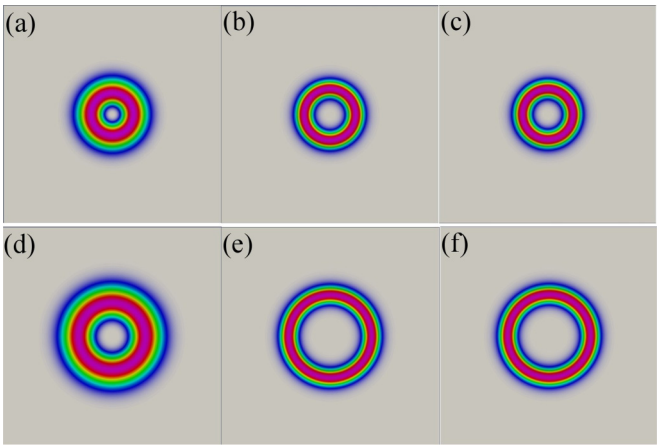

FIG. 2. (Color online) Initial vortices ($z = 0$) for charges $S = 3$ (a) and $S = 5$ (d) correspond to the input parameters $\beta = 0.25$, $\delta = 0.01$, $\mu = 0.4$, and $\varepsilon = 0.45$ from stability region. Vortex solitons are self-generated after respectively $z = 300$ (b) and $z = 500$ (e) steps. They both remain stable after $z = 20\,000$ [see (c) and (f)].

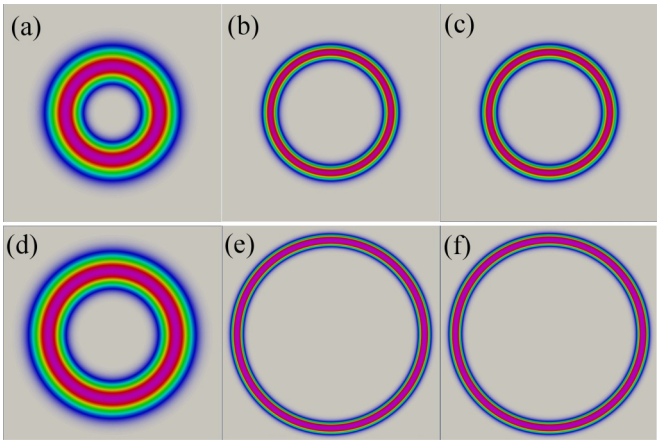

FIG. 3. (Color online) For the same parameters, vortices for $S = 10$ (a) and $S = 20$ (d) become solitons respectively at $z = 1000$ (b) and at $z = 2000$ (e) remaining stable at least till $z = 50\,000$ (c) and $z = 80\,000$ (f).

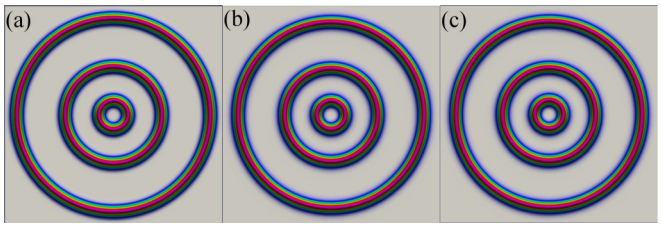

FIG. 4. (Color online) (a) The nesting of $S = 3$ vortex within those of vorticity $S = 10$ and $S = 20$. (b) Propagation distance $z = 100S = 2000$ is necessary for achieving structured self-organization of solitons. (c) Their robustness verified till $z = 50\,000$ allows selective optical tweezing and precise manipulation [20].

$z = 100S$ units. These vortices can coexist simultaneously without mutual interaction as predicted analytically due to imbedding of their stability domains. Indeed, the smallest vortex soliton ($S = 3$) is nested within the larger ones ($S = 10$ and $S = 20$). Such a nesting is set up in the beginning of the numerical evolution (with the same initial conditions as in Figs. 2 and 3 although rescaled) when solitons are not yet formed, as in Fig. 4(a). The vortex soliton with $S = 3$ is self-generated first. The next to be established is the dissipative soliton for $S = 10$, encircled finally by the largest solitonic volcano with $S = 20$. At $z = 2000$ all three dissipative solitons are self-organized [see Fig. 4(b)]. The robustness of the nesting is confirmed by a numerical propagation of up to $z = 50\,000$ [see Fig. 4(c)] without any change in the profiles, as shown in the Supplemental Material [20] for the same parameters $\mu = 0.4$, $\varepsilon = 0.24$, $\delta = 0.01$, and $\beta = 0.05$ as in Figs. 2–4.

The possibility to imbed into the highest charge vortex soliton, solitons with lower vorticity allows selective dynamic tweezing of micro- and nanoparticles [21]. Absorbing particles in gaseous and liquid media may be subjected to photophoretic forces, pushing them away from the regions of high field intensities [22]. Therefore, such particles cannot be trapped by Gaussian beams without singularity ($S = 0$). However, vortex solitons telescoped in a nesting configuration self-generate structured light, making it possible to selectively trap and manipulate noninvasively particles with great precision. Solitons with smaller vorticities can be imbedded gradually in the vortex soliton with the largest charge, and in this manner trap selectively various groups of particles in a nonsimultaneous way and compress them into the ever smaller central region. Such a spatiotemporally structured light may be used as selective dynamic tweezers, in order to characterize the forces exerted by molecular motors such as myosin, kinesin, and ribosomes. Metal-dielectric nanocomposites (MDNCs) composed of either gold or silver nanoparticles (NPs) suspended in liquids, polymers, and glasses are attracting great interest due to their high nonlinear susceptibility [22]. Refractive nonlinearity of NPs can be adjusted by changing their volume fraction. Nested vortex solitons with high topological charge can manipulate dynamically NPs concentration. Therefore, such dynamic tweezers control in real time the spatial distribution of effective nonlinear susceptibility in MDNCs allowing engineering of reconfigurable guides.

In conclusion, we have used a hybrid analytical-numerical approach based on the variational method extended to dissipative systems and parallelized numerical simulations, to develop a cubic-quintic Ginzburg-Landau model resistant to modulational instability, hence, admitting stable localized solitons with high topological charges. An analytical stability criterion is established, allowing determination of stability domains of parameters for vortices with topological charges ranging from $S = 3$ to $S = 20$. It is demonstrated analytically that stability domains of vortices with higher topological charges are nested in areas corresponding to lower vorticity. This indicates the possibility of simultaneous coexistence of vortices with different charges in a realistic experiment [6]. Realistic parameters from these domains, controlled by the laser beam intensity and the choice of active medium, are used as inputs for numerical self-generation of stable dissipative vortex solitons with very high vorticity. The stable and exceptionally robust imbedding of low-vorticity solitons within those with higher values of topological charge is demonstrated. In such a way nanostructured light can be self-generated. Dissipative vortex solitons telescoped selectively in a nesting configuration may be used for dynamic optical tweezing of micro- and nanoparticles as well as for engineering of reconfigurable guides. The main advantage of dynamic selective tweezing realized using nested dissipative vortex solitons would be its exceptional robustness and reproducibility due to the self-organized stabilization.

This publication was made possible by the National Priorities Research Program Grants No. 5-674-1-114 and No. 6-021-1-005 from the Qatar National Research Fund (a member of Qatar Foundation). Work at the Institute of Physics Belgrade is supported by the Ministry of Education and Science of the Republic of Serbia, under Projects OI 171006 and III 45016.

[1] G. Nicolis and I. Prigogine, *Self-organization in Nonequilibrium Systems* (Wiley, New York, 1997).

[2] V. I. Petviashvilli and A. M. Sergeev, Dokl. Akad. Nauk SSSR **276**, 1380 (1984) [Sov. Phys. Dokl. **29**, 493 (1984)]; I. S. Aranson and L. Kramer, Rev. Mod. Phys. **74**, 99 (2002); N. Rosanov, *Spatial Hysteresis and Optical Patterns* (Springer, Berlin, 2002); N. N. Akhmediev and A. Ankiewicz, *Dissipative Solitons: From Optics to Biology and Medicine*, Lect. Notes Phys. 751 (Springer, Berlin, 2008); F. T. Arecchi, S. Boccaletti, and P. L. Ramazza, Phys. Rep. **318**, 1 (1999); F. Lederer *et al.*, *ibid.* **463**, 1 (2008).

[3] B. A. Malomed, Physica D **29**, 155 (1987); S. Fauve and O. Thual, Phys. Rev. Lett. **64**, 282 (1990).

[4] Y. S. Kivshar and G. P. Agrawal, *Optical Solitons: From Fibers to Photonic Crystals* (Academic, San Diego, 2003).

[5] V. Skarka, V. I. Berezhiani, and R. Miklaszewski, Phys. Rev. E **56**, 1080 (1997).

[6] E. L. Falcao-Filho, C. B. de Araujo, G. Boudebs, H. Leblond, and V. Skarka, Phys. Rev. Lett. **110**, 013901 (2013).

[7] V. Skarka and N. B. Aleksić, Phys. Rev. Lett. **96**, 013903 (2006).

[8] A. S. Desyatnikov, Yu. S. Kivshar, and L. Torner, *Progress in Optics*, Vol. 47, edited by E. Wolf (North-Holland, Amsterdam, 2005), p. 291.

[9] V. I. Berezhiani, V. Skarka, and N. B. Aleksić, Phys. Rev. E **64**, 057601 (2001); V. Skarka, N. B. Aleksić, and V. I. Berezhiani, Phys. Lett. A **319**, 317 (2003); V. Skarka, N. B. Aleksić, M. Derbazi, and V. I. Berezhiani, Phys. Rev. B **81**, 035202 (2010).

[10] V. Skarka, N. B. Aleksić, H. Leblond, B. A. Malomed, and D. Mihalache, Phys. Rev. Lett. **105**, 213901 (2010).

[11] V. I. Berezhiani, V. Skarka, and R. Miklaszewski, Phys. Rev. B **57**, 6251 (1998).

[12] T. A. Davydova and A. I. Yakimenko, J. Opt. A: Pure Appl. Opt. **6**, S197 (2004); R. M. Caplan, Q. E. Hoq, R. Carretero-Gonzalez, and P. G. Kevrekidis, Optics Comm. **282**, 1399 (2009).

[13] L.-C. Crasovan, B. A. Malomed, and D. Mihalache, Phys. Rev. E **63**, 016605 (2000); D. Mihalache, D. Mazilu, F. Lederer, Y. V. Kartashov, L. C. Crasovan, L. Torner, and B. A. Malomed, Phys. Rev. Lett. **97**, 073904 (2006); D. Mihalache, D. Mazilu, F. Lederer, H. Leblond, and B. A. Malomed, Phys. Rev. A **76**, 045803 (2007); **75**, 033811 (2007).

[14] N. N. Akhmediev, V. V. Afanasjev, and J. M. Soto-Crespo, Phys. Rev. E **53**, 1190 (1996); J. Atai and B. A. Malomed, Phys. Lett. A **246**, 412 (1998); W. J. Firth and P. V. Paulau, Eur. Phys. J. D **59**, 13 (2010).

[15] S. Chavez Cerda, S. B. Cavalcanti, and J. M. Hickmann, Eur. Phys. J. D **1**, 313 (1998).

[16] N. B. Aleksić, V. Skarka, D. V. Timotijević, and D. Gauthier, Phys. Rev. A **75**, 061802(R) (2007).

[17] V. Skarka, D. V. Timotijević, and N. B. Aleksić, J. Opt. A: Pure Appl. Opt. **10**, 075102 (2008).

[18] E. Ding, K. Luh, and J. N. Kutz, J. Phys. B: At. Mol. Opt. Phys. **44**, 065401 (2011).

[19] B. N. Aleksić, N. B. Aleksić, V. Skarka, and M. Belić, Phys. Scr. **T149**, 014036 (2012).

[20] See Supplemental Material at http://link.aps.org/supplemental/10.1103/PhysRevA.91.043832 for a movie that displays the real dynamics of the self-organized light structuring where the smallest vortex soliton ($S = 3$) is nested by the larger ones ($S = 10$ and $S = 20$).

[21] A. Ashkin, Phys. Rev. Lett. **24**, 156 (1970); Science **210**, 1081 (1980); A. Ashkin, J. M. Dziedzic, J. E. Bjorkholm, and S. Chu, Opt. Lett. **11**, 288 (1986); A. Ashkin, J. M. Dziedzic, and T. Yamane, Nature **330**, 769 (1987).

[22] D. Grier, Nature **424**, 810 (2003); V. Shvedov, A. R. Davoyan, C. Hnatovsky, N. Engheta, and W. Krolikowski, Nat. Photon. **8**, 846 (2014).